J Geod (2014) 88:659–673
DOI 10.1007/s00190-014-0712-1

ORIGINAL ARTICLE

# Precise station positions from VLBI observations to satellites: a simulation study

**Lucia Plank · Johannes Böhm · Harald Schuh**

Received: 17 September 2013 / Accepted: 3 March 2014 / Published online: 23 March 2014


**Abstract** Very long baseline interferometry (VLBI) tracking of satellites is a topic of increasing interest for the establishment of space ties. This shall strengthen the connection of the various space geodetic techniques that contribute to the International Terrestrial Reference Frame. The concept of observing near-Earth satellites demands research on possible observing strategies. In this paper, we introduce this concept and discuss its possible benefits for improving future realizations of the International Terrestrial Reference System. Using simulated observations, we develop possible observing strategies that allow the determination of radio telescope positions in the satellite system on Earth with accuracies of a few millimeters up to 1–2 cm for weekly station coordinates. This is shown for satellites with orbital heights between 2,000 and 6,000 km, observed by dense regional as well as by global VLBI-networks. The number of observations, as mainly determined by the satellite orbit and the observation interval, is identified as the most critical parameter that affects the expected accuracies. For observations of global positioning system satellites, we propose the combination with classical VLBI to radio sources or a multi-satellite strategy. Both approaches allow station position repeatabilities of a few millimeters for weekly solutions.

L. Plank (✉) · J. Böhm
Vienna University of Technology, Gußhausstraße 27-29,
1040 Vienna, Austria
e-mail: lucia.plank@tuwien.ac.at

*Present Address:*
L. Plank
University of Tasmania, Private Bag 37, Hobart 7001, Australia

H. Schuh
DeutschesGeoForschungsZentrum GFZ, Telegrafenberg, A17,
14473 Potsdam, Germany

**Keywords** Very long baseline interferometry · Terrestrial reference frame · VLBI-satellite tracking · Space tie

## 1 Introduction

Observations to distant radio sources with the very long baseline interferometry (VLBI) technique enable the determination of a space-fixed celestial reference frame and the location of the Earth relative to it, in terms of Earth orientation parameters (EOP). VLBI is one of the four space geodetic techniques contributing to the latest realization of the International Terrestrial Reference System, the International Terrestrial Reference Frame 2008 (ITRF2008; Altamimi et al. 2011). Combining observations from VLBI, satellite laser ranging (SLR), the global positioning system (GPS) and Doppler orbitography and radiopositioning integrated by satellite (DORIS), the ITRF optimally utilizes the strengths of each technique. Besides the space geodesy solutions, the ITRF also relies on local ties at co-location sites, establishing the link between the various techniques.

At co-location sites, where two or more space geodetic instruments are located nearby, the geometric vectors between the various reference points are usually determined by classical surveying. This is not a trivial task, as the antenna reference points are either difficult to access or might even change with time (e.g., Sarti et al. 2011). When comparing the measured local tie vectors with the space geodesy results, discrepancies of several millimeters or even more than 1 cm are observed (Altamimi et al. 2011; Seitz et al. 2012). Altamimi et al. (2011) further conclude, that for future improvement of the ITRF the consistency between local ties and space geodesy estimates needs to be improved.

A promising complement to the local ties on Earth is the concept of space ties via co-location satellites. Having

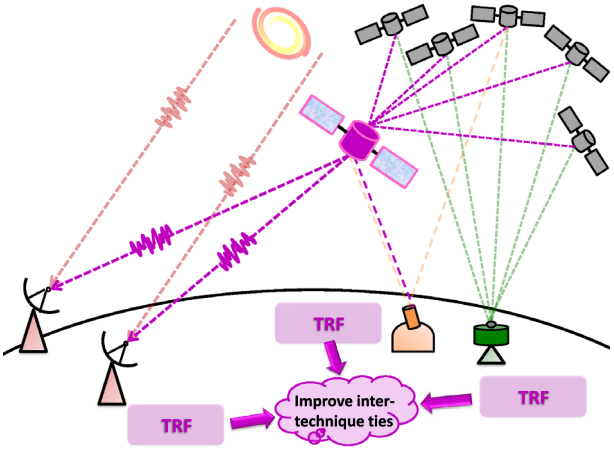


**Fig. 1** A co-location satellite used as a space tie. The tracking by VLBI, SLR and GNSS enables the realization of inter-technique ties and the connection of the three single-technique TRFs

more than one technique sensor available on a satellite, and assuming that the relative positioning of these sensors can be established very precisely, such a satellite would serve as a so-called space tie, combining the different techniques. Using observations to several satellites of the global navigation satellite systems (GNSS) that are equipped with SLR retro-reflectors, Thaller et al. (2011) successfully show the combination of GNSS and SLR via co-location satellites, as an alternative to local ties on ground.

In this paper, we concentrate on co-locations with VLBI. In principle, there are two possible scenarios:

(a) one uses the available geodetic infrastructure, i.e., one observes the signals emitted by the GNSS satellites with VLBI, or
(b) a dedicated new satellite is launched carrying a VLBI transmitter in addition to sensors of GNSS, SLR and DORIS.

The second concept is illustrated in Fig. 1: a satellite, orbiting beneath the GNSS constellation, can be tracked by GNSS, SLR and VLBI. This enables the connection of the three systems, realizing inter-technique ties. While GNSS positioning of a low Earth orbiting satellite and SLR tracking are well-established techniques, the VLBI tracking is rather innovative. Hence, progress in hardware as well as research on the concept itself is required.

The aim of this paper is to investigate the feasibility of observing satellites with VLBI. This includes examinations on common visibilities of satellites at different orbital heights observed with radio telescopes in different networks. With the help of simulated observations, we assess expected accuracies of radio telescope positions on Earth determined by VLBI satellite observations. The derived coordinates in the satellite system could then be compared to those derived in standard VLBI observing radio sources. In that way, a frame tie between the satellite frame and the VLBI frame is established. In Sect. 2, we start with an introduction of VLBI satellite observations, under consideration of several practical issues. In Sect. 3, the simulation approach is described, and the results are presented in Sect. 4. The most important findings are summarized and discussed in Sect. 5.

## 2 VLBI observations to satellites

With VLBI being one of the senior space geodetic techniques, there have been ideas to use this technique for orbit determination of satellites or for Earth surveying right from the beginning (Rosenbaum 1972; Preston et al. 1972; Counselman and Gourevitch 1981). The advance of GNSS and improvements of alternative tracking methods pushed this concept into oblivion, before it was rediscovered in recent years. Using slightly different observing strategies and signals than in geodesy, VLBI, and especially differential (D-)VLBI is a well- established technique commonly used for the navigation of spacecrafts (Lanyi et al. 2007). Following several applications of tracking planetary space probes with a net of geodetic VLBI radio telescopes, as e.g., the descent of the Huygens probe landing on Saturn's moon Titan (Lebreton et al. 2005), Duev et al. (2012) introduced the Planetary Radio Interferometry and Doppler Experiment (PRIDE). Enabling ultra-precise estimation of spacecraft state vectors using the imaging technique with a multi-station network, PRIDE might be also applicable for near-Earth targets, as GNSS satellites (Duev et al. 2012). In the course of developing VLBI tracking to the lunar probes SELENE and Chang'E, Japanese and Chinese tracking teams tested the mostly newly developed hardware and software also with observations to near Earth orbiters and satellites (e.g., Hanada et al. 2008; Huang et al. 2006). Following successful applications in space missions, now there are plans to use VLBI tracking for precise orbit determination of geostationary satellites, e.g., of China's COMPASS satellite navigation system (Huang et al. 2011).

In geodesy, and disregarding the immediate goal of orbit determination, the driving force behind is the improvement of reference frames. In particular, the tie between the quasi-inertial International Celestial Reference Frame (ICRF) and some TRFs, as e.g., determined by space geodetic techniques, is of interest. This interaction is the topic of the IAG Sub-Commission 1.4[1] with one of its objectives to analyze VLBI observations to GNSS satellites and to simulate future micro satellite missions like GRASP in VLBI analysis software. Hase (1999) proposed the observation of GPS satellites with VLBI, with the goal to tie the satellite transmit-

[1] http://iag.geo.tuwien.ac.at.

**Table 1** Main differences between VLBI observations to extragalactic radio sources (quasars) and those to transmitters aboard a satellite

| | Quasars | Satellite targets |
|---|---|---|
| Target position | Fix w.r.t. the ICRF | Moving source |
| | | Erroneous positions due to orbit errors |
| Signal | Continuous spectrum | Artificial signal at distinct frequencies; limited bandwidth |
| | Weak signal | Strong signal |
| Receiving system | Standard (geodetic) VLBI system | Modifications necessary e.g., for observations at L-band |
| Common visibility | Long baselines | Limited visibility for low satellites |
| Tracking | Automated correction for Earth's rotation | Following the satellite |
| | | E.g. SATTRACK (Moya Espinosa and Haas 2007) |
| Field system | Standard (geodetic) VLBI field system | Modification for satellite targets |
| | | New data formats |
| Modeling | Plane wavefront | Curved wavefront |
| | Infinite distance | Light time iteration for time of emission |

ters of the GPS directly to the ICRF. Such involvement of satellites in VLBI would also enable access to the Earth's center of mass determined in the ICRF, which is not possible with classical VLBI (Dickey 2010). With VLBI tracking of GLONASS satellites at L-band, Tornatore et al. (2011) successfully demonstrated the technical realization of such observations. Further developments in that area are expected. Representative for several possible upcoming missions currently discussed, e.g MicroGEM at GeoForschungsZentrum Potsdam[2] (Brieß et al. 2009), we mention here the Geodetic Reference Antenna in Space concept (GRASP; Bar-Sever et al. 2009). GRASP is a mission proposal following the second concept introduced above, of a dedicated new satellite with the goal to realize a space-tie to improve future TRF realizations. Building on a different way of operation but worth to mention in this context is the GPS-VLBI hybrid system (Kwak et al. 2010), where GPS signals received by standard GPS antennas are recorded and correlated in VLBI mode, enabling the combination of GPS and simultaneously recorded VLBI data at observation level.

Though not the main topic of this paper, some words are given on the technical realization of such observations. In particular, we work out some areas in which observations to transmitters aboard an Earth-orbiting satellite differ from VLBI observations to extragalactic radio sources, mainly quasars. An overview of these main differences is shown in Table 1.

Most evident is the fact, that while the position of a quasar is fixed w.r.t. the ICRF, the target satellite is constantly moving and its position has to be determined carefully. In geodetic VLBI, errors due to positional changes of the quasar as an effect of source structure are small and are usually neglected. When observing a satellite, precise orbit determination is an important issue. On the one hand, VLBI observations might support the orbit determination itself, while on the other hand, orbit errors effect the VLBI observations and may distort the derived products. In this paper, we neither estimated satellite positions with VLBI nor investigated the effect of orbit errors on the determined positions of the radio telescopes. Compared to classical VLBI, where random noise emitted by natural radio sources is observed, the signal emitted by satellites has to be generated artificially. While in radio source VLBI, the measurement precision is achieved through the use of broad-band signals, a signal from an artificial source is mostly limited in bandwidth. This fact necessitates the transition to phase delays instead of group delays or to identify alternative methods to reach sufficient precision of the measured quantity. When making use of signals not originally designated for VLBI tracking, observations in other frequency domains than in the standard S-/X-band might be necessary. In the case of GNSS, observing the strong L-band signals requires the use of receiving systems matching the corresponding frequency and signal strength, instead of the common receivers that are optimized for S-/X-band observations of the extremely weak signals emitted by extragalactic radio sources. Investigations on the observability of GNSS signals were done e.g., by Hase (1999) and Tornatore and Haas (2009). The latter ones conclude, that for observations of GNSS signals with the future VLBI2010 system it should be possible to determine group delays for GNSS signals with a precision on the order of 1 cm or better.

There is an additional obstacle that needs to be mentioned here and came up when Working Group 1 of the International VLBI Service for Geodesy and Astrometry (IVS; Schuh and Behrend 2012) discussed the feasibility of using VLBI for

[2] MicroGEM is a feasibility study for future GNSS-remote sensing satellites of the GeoForschungsZentrum (GFZ) Potsdam. The concept, that in the meanwhile has been prolonged under the names "NanoGEM" and "NanoX", also includes a VLBI transmitter aboard the satellite.

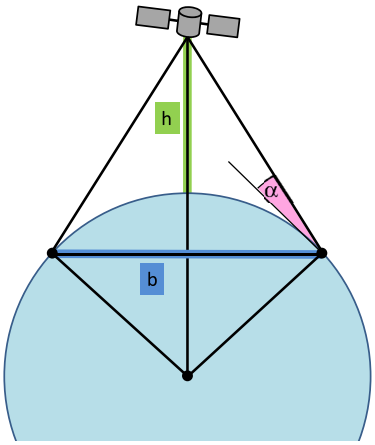


**Fig. 2** Geometry for the calculation of common visibility, using the satellite orbital height $h$, the baseline length $b$ and the maximum common elevation angle $\alpha$

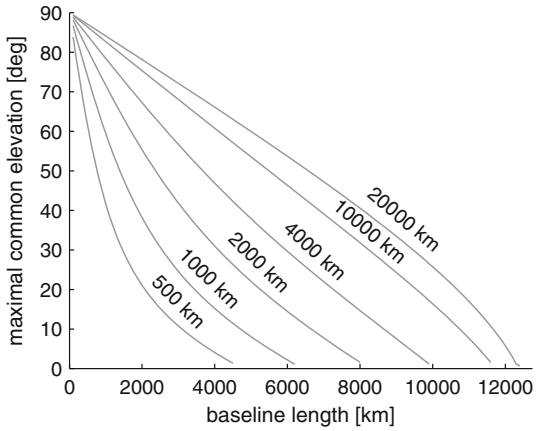


**Fig. 3** The maximum common elevation angle for different baseline lengths and in dependence of the satellite orbital height, following the geometry of Fig. 2

GPS phase center mapping[3]. It is related to the fact that the GPS signal, enabling a beam coverage of the whole globe, is generated in a phased antenna array rather than ideally transmitted from a compact antenna. As a consequence, the signals received at different VLBI radio telescopes are not leaving the transmitter aboard the GPS satellite with identical phase from one center. Any possible transmitter signal modeling errors were not included in our study.

The questions of common visibility of the target satellite and its tracking by the receiving antennas are discussed in Sects. 2.1 and 2.2.

The last point mentioned in Table 1 concerns the modeling of the VLBI observations. In classical VLBI using quasars, the sources are billion of light years away and the signal arrives as plane wave front at the Earth's surface. This is not true for close satellite targets, where the curvature of the wave front must be included in the model. In addition, to determine the position of the target satellite at the time of signal emission, a so-called light time iteration between the receiving and emitting epochs has to be performed. More details on the modeling are given in Sect. 3.

### 2.1 Common visibility

Simultaneous visibility by at least two radio telescopes is an essential prerequisite for VLBI observations. Decisive parameters therefore are the orbit of the target, first and foremost the satellite orbital height, and the network of the observing radio telescopes. The relation of satellite orbital height and baseline length is determined following the geometry given in Fig. 2. The maximum separation between the two stations (baseline length $b$), where a satellite at orbital height $h$ can still be observed is found for a satellite above the midpoint of the baseline. The maximum elevation angle at which the satellite can be observed by the two stations is depicted by $\alpha$. In Fig. 3, the relation between elevation $\alpha$, baseline lengths from 100 km up to the Earth's diameter and six selected satellite orbital heights between 500 and 20,000 km is illustrated. A satellite at 2,000 km can be observed from two stations with a maximum separation of 8,000 km, though under very low elevation of a few degrees only. For a cut-off elevation of 15°, a maximum baseline length of 6,000 km is possible.

### 2.2 Antenna slewing

In geodetic VLBI, the pointing direction of an antenna needs to be corrected for the Earth's rotation during an observation at a maximum rate of 0.25°/min. More important is a fast switching between sources that are well distributed on the sky. While the currently used VLBI system within the IVS includes antennas with slew speeds of about 0.4°–3°/s, the target for the next generation VLBI system, the upcoming VLBI2010 Global Observing System (VGOS; Hase et al. 2013), is at 6°–12°/s (Schuh and Behrend 2012).

When observing satellites, the VLBI antenna has to follow the target on its way through the sky. Alternatively, when the observation duration is short, the observation can be performed with the antenna being fixed and the satellite passing through the antenna beam. While the tracking normally should not be a problem for the quite slow satellites of the GNSS (Tornatore and Haas 2009), in the case of lower satellites, fast antennas are required. For a precise calculation of the necessary slewing times, the duration of the observation as well as the individual capabilities of each antenna have to be considered, as e.g., described in Sun (2013). Especially close to zenith, the necessary azimuthal slew rates grow rapidly and possible singularities have to be considered. For

[3] The discussion of IVS WG 1 is available at: http://ivscc.gsfc.nasa.gov/about/wg/wg1.

the simulated schedules investigated in this paper, the observation duration was assumed to be very short, i.e., without considering any scan length. Antenna slewing was not explicitly investigated. For the practical realization of VLBI satellite observations, also the field system of the radio telescope as well as the standardized data exchange formats have to be amended accordingly. In terms of satellite tracking itself, this can be done e.g., using a module called SATTRACK (Moya Espinosa and Haas 2007), enabling the antenna to follow the satellite on its path trough the sky.

## 3 Simulation study

The simulation study described in this paper was set up as follows (Fig. 4): after constructing a schedule of observations (Sect. 3.1) for seven consecutive days, the observations were simulated as described in Sect. 3.2. To get a representative sample, the simulations, which are partly based on random numbers, were repeated 30 times. The results of these simulations are observed minus computed ($o-c$) values, that were the input for the least-squares estimation tool. The derived normal equation matrices for 7 days were then combined in a global solution, where parameters were determined in a weekly solution. Following the usually applied strategy of daily sessions, this enabled the processing of observations for a seamless 7-day period. From the sample of 30 weekly solutions, applying statistical analysis according to Sect. 3.4, the final results in terms of station position repeatabilities were derived.

For the simulation study, the Vienna VLBI Software (VieVS; Böhm et al. 2012) was used. Therefore, the software was extended by the possibility of processing satellite VLBI data, with all necessary amendments united in the general heading $VieVS_2tie$. The main changes include the treatment of satellite orbits given in some TRF, either in simple ASCII tables or as sp3-files in the case of GNSS, and the according delay model for sources at finite distances. In $VieVS_2tie$, the model for VLBI observations of Earth satellites suggested by Klioner (1991) was implemented, with all calculations performed in a geocentric system rather than in a barycentric one. Another necessary step is the calculation of the time of signal emission at the satellite $t_0$, which has to be calculated iteratively solving the light time equation. As e.g., described in Moyer (2003), first the signal travel time is calculated between the satellite and the receiver at the receiving epoch at station 1 $t_1$, accounting for the straight-line distance as well as for the relativistic light time. Subtracting this signal travel time from $t_1$ gives the first approximation for $t_0$. Then, the signal travel time is repeatedly calculated between the satellite's position at $t_0$ and the receiving telescope at $t_1$, generating new values for $t_0$ each run. Usually, a few iterations of this process are sufficient. Enabling the common processing of observations to satellite targets and extragalactic radio sources, a new data format was created, including the observation type. Consequently, when the type says $qq$ for the classical quasar observation, the standard processing is chosen, whereas for type spacecraft $sc$, the new processing chain of $VieVS_2tie$ is run. $VieVS_2tie$ in principle is capable to process real VLBI observations to satellites as given in terms of time delays. Due to the lack of available data, the verification of the developed software with real observations is still pending.

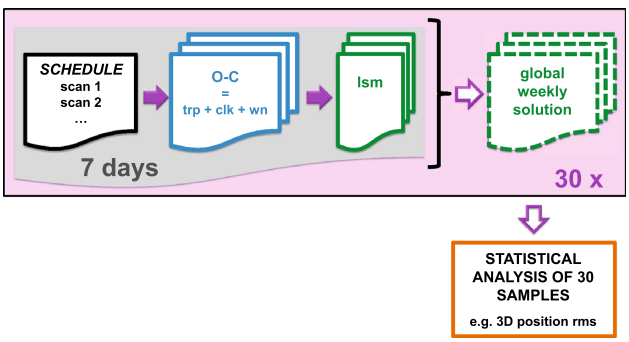


**Fig. 4** Simulation setup. Observations were scheduled for 7 consecutive days and simulated 30 times. In the lsm-tool, the normal equation matrices were set up which were then analyzed in weekly global solutions. The sample of 30 repetitions allows for a statistical analysis that can be interpreted as expected accuracies for the derived parameters

### 3.1 Scheduling

Observations were scheduled to three different satellites, with the orbital parameters given in Table 2. Satellite S2 was designed following an initially planned orbit of the proposed GRASP mission, flying at 2,000 km orbital height. The orbit design of satellite S6 matches the one of the LAGEOS 1 satellite, with a nominal orbital height of 6,000 km. As a third approach, GPS satellites were used for our studies, with orbital heights of about 20,200 km.

Concerning the antenna network, we considered dense and regional networks as well as global ones. Based on existing VLBI radio telescopes, but disregarding the functionality for tracking satellites, three regional networks were defined according to Fig. 5. A European network (EUR)

**Table 2** Orbital parameters of the target satellites

| | S2 | S6 | GPS |
|---|---|---|---|
| Orbital height | 2,000 km | 6,000 km | ~20,200 km |
| Inclination | 104.89° | 109.84° | ~55° |
| Eccentricity | 0.0001 | 0.0334 | Nearly circular |
| Orbital period | ~130 min | ~225 min | ~12 h |

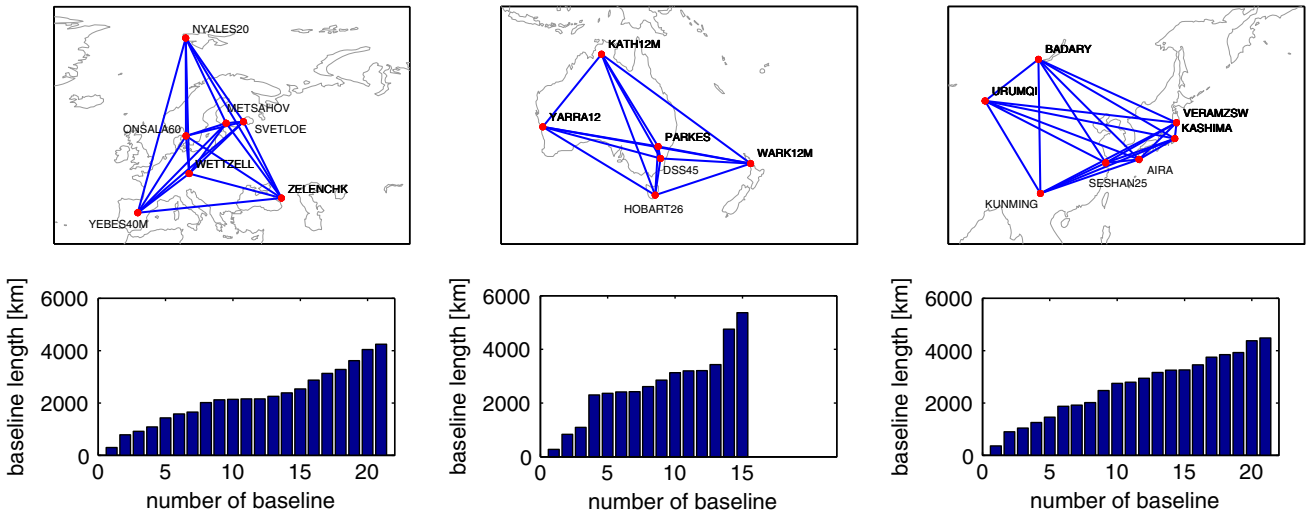


**Fig. 5** Baselines in the regional networks EUR (*left*), AUS (*middle*), and ASIA (*right*). The corresponding baseline lengths are given below each network

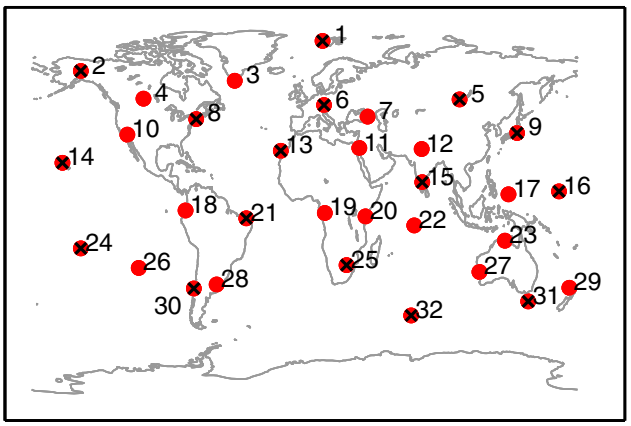

**Fig. 6** Global networks of real and fictitious stations. *Red dots* indicate the 32 stations of the large network and the *black crosses* mark the 16 stations of the smaller network. The *numbers* of the stations correspond to those of Fig. 11

with antennas in Ny-Ålesund, Metsähovi, Onsala, Svetloe, Wettzell, Yebes, and Zelenchukskaya, seven antennas in Asia (ASIA), namely Aira, Badary, Kashima, Kunming, Mizusawa, Shanghai and Urumqi, and the AUS network in the Australian/Oceanian region with DSS45, Hobart, Katherine, Parkes, Warkworth, and Yarragadee.

In Fig. 5, lower plots, the distribution of baseline lengths for the three networks is shown. The majority of the formed baselines has a length of 2,000–3,000 km that—according to Fig. 3— should enable common visibilities also for the S2 satellite.

For the simulation of global networks, we used fictitious networks of the VLBI2010 simulations, as proposed by Niell (2007). The advantage of these networks is a homogeneous global distribution of antennas, including existing and hypothetical stations. Observations were scheduled for the two global networks of Fig. 6, one with 16 stations (black crosses) and one with 32 stations (red dots). The scheduling itself was simply based on common visibilities, disregarding antenna specifications, signal strengths or slewing times. The input parameters were the satellite orbit and the antenna network, the observation interval and the cut-off elevation angle $\mathrm{el}_{\mathrm{min}}$. Both parameters had to be chosen with care, especially when the total number of observations was small, e.g., through limited common visibilities.

### 3.2 Simulated observations

Simulations are performed to approximate real data, allowing to draw conclusions that are transferable to reality. Therefore, the behavior of real observations has to be abstracted through a realistic model, and a suitable simulation method must be chosen. The simulator of the VieVS (Pany et al. 2010; Petrachenko et al. 2009) was used, comprising the three most important stochastic error sources in VLBI, namely wet troposphere delay, station clock, and measurement errors. Pany et al. (2010) give a detailed description on these simulations and, using a sample of 25 repetitions, justify its applicability through comparisons with real observations.

We used Monte Carlo simulations, which simulate the above-mentioned errors on the basis of models and random numbers. The sample of 30 repetitions allowed a subsequent statistical interpretation of the results, e.g., in terms of mean values or variance. The simulations were set up as follows: for each observation, the effects of the wet troposphere $\tau_{\mathrm{trp}}^{12}$, the station clocks $\tau_{\mathrm{clk}}^{12}$, and a measurement noise $\tau_{\mathrm{wn}}^{\mathrm{bl}}$ were calculated following adequate models. Tropospheric delays $\tau_{\mathrm{trp}}^{\mathrm{i}}$ were calculated per station

**Table 3** Parameters used to simulate observations, following the method described in Pany et al. (2010)

| | |
|---|---|
| Clock | |
| Allan standard deviation | $1 \times 10^{-14}$ @50 min |
| Tropospheric turbulence | |
| Initial zenith wet delay | 150 mm |
| Structure constant $C_n$ of a turbulent troposphere | $2.0 \times 10^{-7}$ m$^{1/3}$ |
| Effective height of the troposphere | 2 km |
| Wind speed in eastern direction | 8 m/s |
| Wind speed in northern direction | 0 m/s |
| Height increment for integration | 200 m |
| Correlation interval | 8 h |
| Measurement error | |
| White noise | 30 ps |

**Table 4** Processing options for the analysis of the simulated observations

| | |
|---|---|
| Earth orientation | |
| Parameters | Fixed |
| Troposphere | |
| Zenith wet delays | 30 min piecewise linear (pwl) offsets |
| | 1 cm relative constraints |
| | No gradients |
| Clock | |
| | 60 min pwl offsets |
| | + rate + quadratic term |
| | 1.3 cm relative constraints |
| Station coordinates | |
| | NNT, NNR applied |

($i = 1, 2$) following Nilsson et al. (2007). Clocks (clk) were modeled for each station ($i = 1, 2$) as sum of a random walk and integrated random walk, and for the measurement error white noise (wn) was assumed per baseline (bl). The characteristic numbers for the models are given in Table 3.

The simulation was repeated 30 times using new random numbers for each run. We checked some of our simulations using a sample of up to 100 repetitions. The station position repeatabilities were identical at the sub-millimeter level with those that were achieved with the sample of 30 repetitions. Assuming that there are no further error sources, the sum of the simulated effects forms the observed minus computed values $o - c$, which were then used in the estimation process.

$$o - c = \tau_{\mathrm{trp}}^{12} + \tau_{\mathrm{clk}}^{12} + \tau_{\mathrm{wn}}^{\mathrm{bl}} \tag{1}$$

The simulated observations, or rather the $o - c$ values, do not directly depend on a dedicated delay model for calculating the geometrical time delay. Although implemented in the software, the theoretical delay that accounts for a curved wavefront and considers the movement of the target satellite cancels when comparing the simulated (observed) values with the modeled ones. The information about the geometry and the modeled delay is kept in the partial derivatives of the observable with respect to the target parameters, e.g., the station's position.

### 3.3 Processing

The simulated observations were analyzed with $VieVS_2tie$. The processing options concern the parameterization of the least-squares adjustment. Standard VLBI processing options were applied, with some exceptions and specifications as given in Table 4. EOP were not estimated in the analysis. When doing so, the effect on the results was negligible (<1 mm). Zenith wet delays (zwd) were estimated as piecewise linear (pwl) offsets every 30 min for each station. During estimation and especially important at periods without observations, constraints of 1 cm after 30 min were applied. Troposphere gradients to address azimuthal asymmetry were not estimated. The clocks were set up as 60 min pwl offsets, plus a rate and a quadratic term, with 1.3 cm constraints after 60 min. For estimating station coordinates, a datum has to be defined. We set the datum on all stations by applying a no-net-rotation (NNR) and no-net-translation (NNT) condition.

In this work, the approach of weekly solutions was chosen. This is a common strategy in TRF calculation, as e.g., the services for SLR and GNSS deliver weekly solutions of station coordinates (as of 2013). Also the GRASP proposal (Bar-Sever et al. 2009) followed this concept. For the VLBI satellite observations, predominantly due to the limited number of observations, solutions for antenna coordinates over 7 days are more stable than coordinates after 1 or 2 days. Our investigation on this matter showed improvements of more than a factor of two when going from a 1-day solution to a weekly solution.

### 3.4 Station position repeatability

The parameter that was used to assess the simulation results is the repeatability of antenna coordinates, named 3D position rms in the following. Starting from seven daily sessions, each simulated 30 times, we got 210 sessions for each schedule. In the global solution, seven consecutive days were combined and one set of antenna coordinates ($\mathrm{d}x, \mathrm{d}y, \mathrm{d}z$) was estimated for each station, repeated 30 times. For a better geometrical interpretation, $\mathrm{d}x$, $\mathrm{d}y$, and $\mathrm{d}z$ were converted to local up-($\mathrm{d}r$), east-($\mathrm{d}e$) and north-($\mathrm{d}n$) components. The standard deviation $\sigma$ of these estimates gives a measure of the expected accuracy of derived antenna coordinates. The standard deviation $\sigma_{\mathrm{d}r}$

for $n = 30$ samples with the mean value $\mathrm{d}r_m$ was calculated as:

$$\sigma_{\mathrm{d}r} = \sqrt{\frac{1}{n-1}\sum_{i=1}^{n}(\mathrm{d}r_i - \mathrm{d}r_m)^2}. \quad (2)$$

The 3D position rms was defined as:

$$3\mathrm{Drms} = \sqrt{\sigma_{\mathrm{d}x}^2 + \sigma_{\mathrm{d}y}^2 + \sigma_{\mathrm{d}z}^2} = \sqrt{\sigma_{\mathrm{d}r}^2 + \sigma_{\mathrm{d}e}^2 + \sigma_{\mathrm{d}n}^2}. \quad (3)$$

As will be shown in the results in Sect. 4, the number of observations for an individual station is often highly correlated with the accuracy. The number of observations per day was defined as the mean value per station:

$$n_{\mathrm{obs}} = \mathrm{mean}\left(n_{\mathrm{obs}}^{\mathrm{day1}} \ldots n_{\mathrm{obs}}^{\mathrm{day7}}\right). \quad (4)$$

## 4 Results

The station position repeatabilities obtained from observations of satellite S2 and S6 with regional networks are presented in Sect. 4.1. The results give some insight in the influence of scheduling options and the total number of observations. We assessed the reliability of our simulations and discuss the impact of the simulation and processing parameters. In Sect. 4.2, results from observations in global networks are presented. For the case of GPS observations, alternative observation strategies are required, and two concepts are proposed in Sect. 4.3.

### 4.1 Regional networks

In Fig. 7, the station position repeatabilities are shown if satellite S2 and S6 were observed in the EUR, AUS and ASIA networks. The results are given in weekly 3D position rms (orange) as well as in up-(blue), east-(green) and north-(brown) component. In addition, the number of observations per station is illustrated. Overall, we can say that with VLBI observations to satellite S2 or S6, observed in regional networks, station positions can be determined with accuracies of mostly better than 10 mm. The results for the lower satellite S2 are better than for satellite S6, with the best results of 5 mm mean weekly 3D position rms for the EUR network. The slightly worse results for the AUS and ASIA network are due to a lower number of observations, caused by the generally longer baselines. The baseline lengths are shown in Fig. 5, lower plots. On further inspection, we see that especially for the S2 observations, the errors in north direction are considerably smaller than in the other two components. This is thought to be connected with the satellite orbit with its high inclination. The satellite's main movement is in north–south direction, resulting in a higher sensitivity in this component. In general, the sensitivity of the VLBI measurements is determined by the orientation of the baseline and the position, respectively, the change of position over time, of the target satellite. In addition, large errors in the height components are due to the high correlation between the estimated troposphere zenith wet delays and the station heights. For isolated stations that are located at the edges of the network, e.g., Zelenchukskaya (ZEL) and Yebes (YEB) in the EUR network, or Kunming (KUN) in the ASIA network, we see large errors also in the horizontal components. These stations only form baselines in more or less one direction (see upper plots of Fig. 5).

Figure 7 shows that, in general, stations with more observations are slightly better determined than stations with less observations. When comparing all station repeatabilities of Fig. 7 with the mean number of observations for the corresponding station, a clear correlation was found. However, the positive influence by just increasing the number of observations is limited. When increasing the number of observations $n$, one would expect an improvement of the derived standard deviation $\sigma$ compared to the accuracy of a single observation $\sigma_i$. For observations which are completely uncorrelated and dominated by random Gaussian noise, the derived standard deviation $\sigma$ improves by the square root of $n$:

$$\sigma = \frac{\sigma_i}{\sqrt{n}} \quad (5)$$

This is not true for our observations. Observations that are close in time and space are affected by the similar troposphere and hence, such observations do not give new information. In Fig. 8, we show the relation of weekly 3D position rms versus the number of observations in the EUR network observing satellite S2 (up) and satellite S6 (bottom). Each station is represented by a colored line. Testing different observation intervals, each marker represents the corresponding mean number of observations per day for this station. For comparison, the square-root-of-$n$-law (Eq. 5) is shown in gray. We learn that, at a certain point, a sheer increase of observations did not improve the result any more. When testing different observing intervals, an improvement could be seen when decreasing the interval from 5 to 1 min (S2) or from 10 to 5 min (S6), while no clear further gain was observed for a shorter interval. For consistency, the standard observation interval for observations to both satellites, S2 and S6, was set to 1 min.

Also, strongly connected to the number of observations was the search for the optimum elevation cut-off angle. MacMillan and Ma (1994) suggest 7°–8° as cut-off angle for VLBI. For the satellite observations, cut-off angles of 5°, 7°, 10° and 15° were tested, partly causing a dramatic loss of observations for a high cut-off angle. The best trade-off was found at 10°, which was determined as the standard cut-off angle throughout the results presented in this paper.

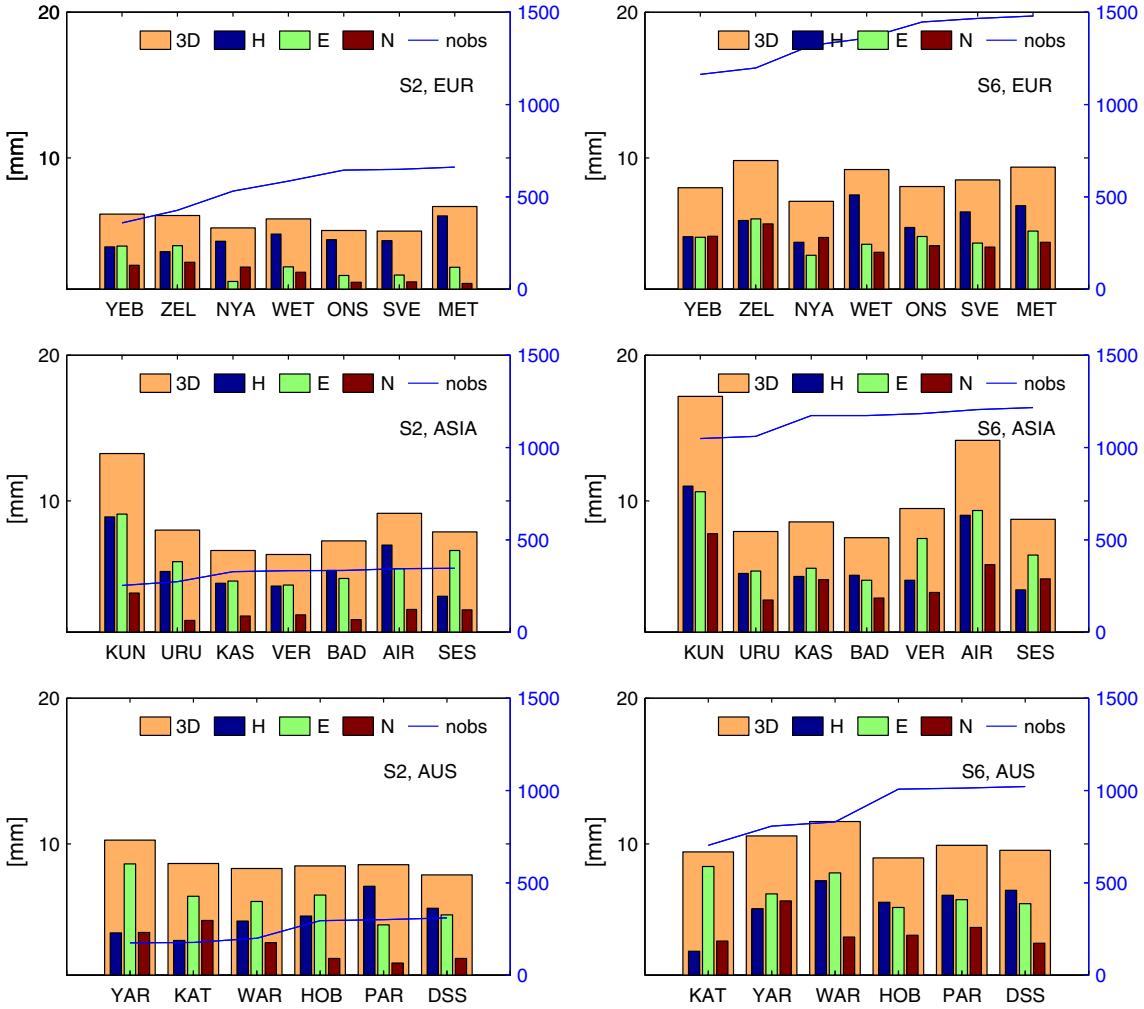


**Fig. 7** Station position repeatabilities in terms of weekly 3D position rms (*orange*) as well as in up-(*blue*), east-(*green*) and north-(*brown*) component if satellite S2 (*left plots*) and satellite S6 (*right plots*) were observed in the EUR, ASIA and AUS networks. The observations were scheduled in 1 min intervals with a cut-off elevation angle of 10°. The *blue line with the scale on the right* gives for each station the mean number of observations per day (nobs)

Our results are based on simulations. In this paragraph, we want to clarify, how large the influence of the simulation parameters and the processing options is. This was tested with observations in the EUR network. We start with the simulated errors on the observations. In accordance with Pany et al. (2010), we found that the effect of the clock and the measurement error is small compared to the tropospheric disturbances. For the clocks, the assumed Allan standard deviation (ASD) of $1 \times 10^{-14}$ @50 min is rather conservative. Today's hydrogen masers are mostly better than that, but clocks with better ASD did not improve the derived 3D position rms. Concerning the measurement errors, we chose to simulate white noise of 30 ps, which is the delay precision achieved in today's geodetic VLBI (Schuh and Behrend 2012). This also corresponds to the delay precision expectations for observations to GNSS satellites, as given by Tornatore and Haas (2009). We found that the results are rather invariant (1–3 mm degradation) up to a white noise of 80–100 ps, while they rapidly degrade at the centimeter level for noise bigger than that. Difficult to choose was the assumed structure constant of the turbulent troposphere $C_n$, which is dependent on the station location and the actual weather conditions. We ran the simulations with rather high $C_n$ of $2.0 \times 10^{-7}$ m$^{1/3}$. Repeating the simulations for different $C_n$, we can conclude that the results improved by 1–2 mm for very dry conditions (e.g., $C_n$ = 1.0), but they degraded (by 2–3 mm) for extremely wet and turbulent conditions (e.g., $C_n$ = 3.5). The sample of 30 repetitions allowed for statistical interpretation. As already mentioned in Sect. 3.2, Pany et al. (2010) used a sample of 25 and a larger sample did not change our results by more than 1 mm.

The simulation studies presented in this work concentrate on the derivation of antenna positions on Earth in the sys-

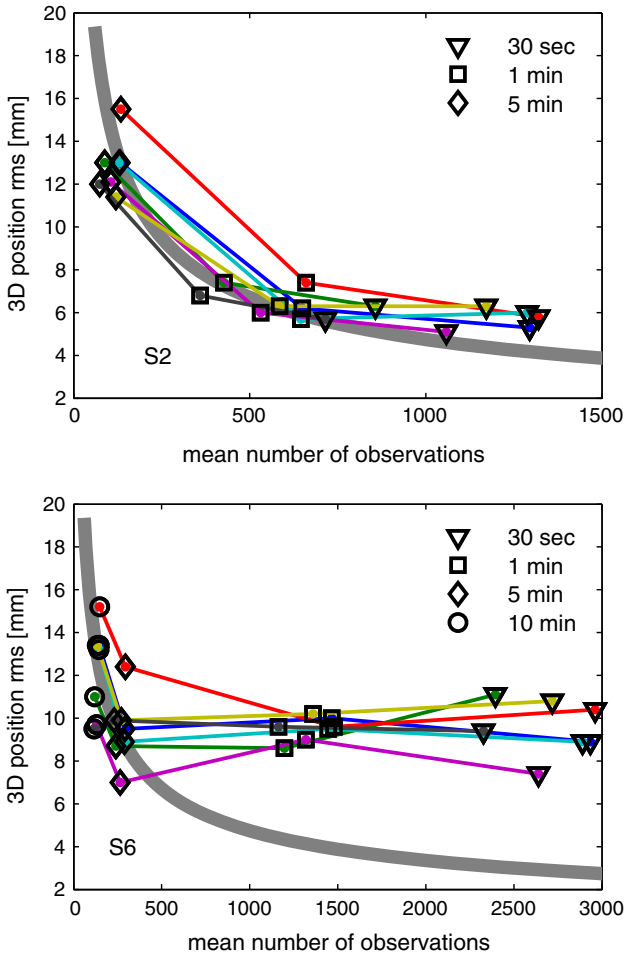


**Fig. 8** Weekly 3D position rms versus the mean number of observations per day. Observations were done with the EUR network to satellites S2 (*up*) and S6 (*bottom*). The *colored lines* represent one station each, with a marker for the number of observations for different observing intervals. For satellite S2, intervals of 5, 1 min and 30 s were tested; in the case of satellite S6, the intervals were 10, 5, 1 min and 30 s. The *gray line* shows the expected improvement according to the square-root-of-*n*-law (Eq. 5)

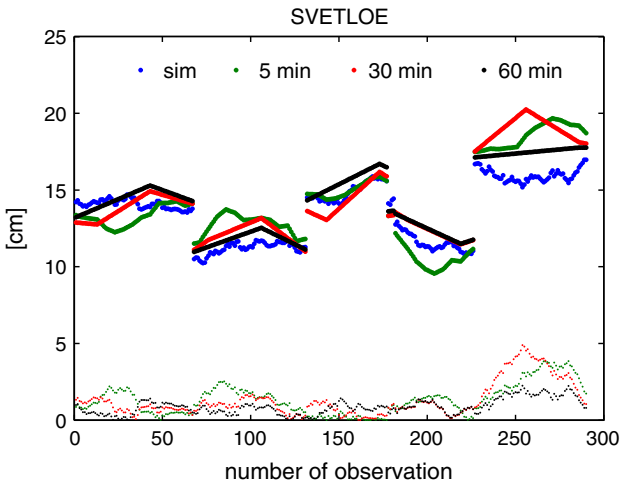


**Fig. 9** Comparison of the simulated zwd (*blue*) and the estimated ones at station Svetloe observing satellite S6 for 1 day in the EUR network. The observation interval was 1 min and the estimation interval for the zwd was 5 min (*green*), 30 min (*red*), and 60 min (*black*). The estimated values were interpolated to the observation epochs. The satellite was observed during five passes and the discontinuities mark the observation gaps between these passes. Besides the total values printed with the bigger markers, the small dots represent the absolute deviation from the simulated values

tem of the observed satellite. The orbit of the satellite was assumed to be perfectly known and orbital errors were not included in our simulations. Further, we concentrated on the derivation of station positions and we did not estimate corrections to the satellite's position.

Concerning changes of the processing options given in Table 4, the only parameter found to significantly influence the results is the estimation interval for the zenith wet delays. For the satellite observations with the EUR network, we varied the estimation interval between 3 min and 3 h, revealing a slightly different behavior for the S2 satellite than for S6. In the case of satellite S2, the estimation interval of 30 min revealed the best results, with marginally worse results (1–2 mm) for shorter or longer estimation intervals. For satellite S6, the effect in weekly 3D position rms was up to 4 mm, when the estimation interval for the zwd was varied between 3 min and 3 h. In general, we found that the zenith wet delays are not determined very accurately in the satellite VLBI observations. In Fig. 9, the simulated zwd as well as the estimated ones using an estimation interval of 5, 30, and 60 min are shown for the station Svetloe observing satellite S6 for 1 day. Differences of up to a few centimeters were found. Repeating this comparison for all stations of the EUR network and with all three estimation intervals, mean deviations of the estimated values from the simulated ones were 0.5 cm for satellite S2 and 0.9 cm for satellite S6. As can also be seen in Fig. 9, none of the estimation interval revealed clearly better results than the others. Further, comparisons of days with bad agreement between the simulated and the estimated zwd with large estimated position offsets did not show a clear relation. In this context, the regional approach and the applied NNT and NNR conditions might be of importance.

Finally, the default constraints of 1 cm after 30 min were reassessed. Constraints of 10 cm and 3 mm, each after 30 min were tested, also using different estimation intervals. The results in terms of weekly 3D position rms changed by up to 2 mm for observations to satellite S2 and up to 7 mm in the case of satellite S6. We can conclude, that the choice of the estimation interval together with the applied constraints has to be done carefully. Further, adjusting the estimation interval dynamically to the actual length of the satellite pass,

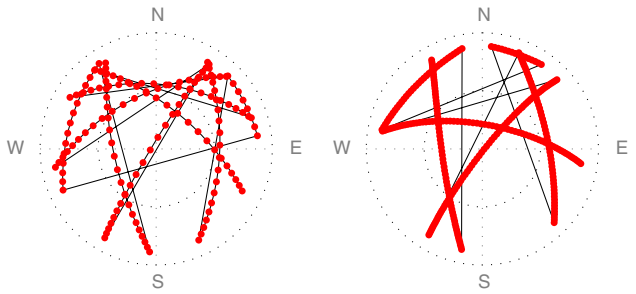


**Fig. 10** Distribution of the observations during 1 day for station Onsala if satellite S2 (*left*) and satellite S6 (*right*) were observed in the EUR network with 1 min intervals. The *black lines* connect consecutive observations

i.e., the time interval when the satellite is visible for at least two stations simultaneously, might be an option.

The fact that despite such big errors in the zwd weekly 3D position rms of a few millimeters could be achieved, is due to the multiple satellite passes. They seem to stabilize the solution for radio telescope positions. While in classical VLBI, one can influence the expected accuracies through a careful choice of the observed sources, when observing a satellite, the observations are arranged following the satellite track. In Fig. 10, the distribution of the observations during 1 day is shown for station Onsala, observing satellite S2 (left) and satellite S6 (right), respectively. The satellites' tracks of each pass can be seen clearly.Running solutions with a reduced number of satellite passes showed that the solution stabilized when the satellite was observed for at least three passes, with only marginal further improvement when more passes were included.

### 4.2 Global networks

Keeping in mind the promising results for observations with regional networks, we also tested the performance in global networks. Therefore, the station position repeatabilities were calculated if satellite S2 and S6 were observed in the fictitious 32/16 stations networks. In addition, the three regional networks EUR, ASIA, and AUS were combined to a global cluster network. This should ensure a sufficiently dense network on the one hand and a global network without increasing the number of antennas too much on the other. In Table 5, the mean weekly 3D position rms is given. Figure 11 shows the results if satellite S2 was observed in the 32 stations network, satellite S6 in the 16 stations network and both satellites observed in the cluster network. For satellite S2, a global network of 16 stations revealed a mean weekly 3D position rms of 32 mm and seems not adequate. When the number of stations was doubled, the results are on the level of 10–30 mm, with a strong dependence on the number of observations (Fig. 11). While for stations with many observations the results are nearly as good as for the regional networks, for stations with a low number of observations (<400) the rms values are large. We see that for most stations the height errors dominate the horizontal positional accuracy, indicating that the troposphere was not determined sufficiently well. Again, the north component was determined best.

**Table 5** Results in terms of mean weekly 3D position rms if satellite S2 and S6 were observed in the 32 stations, 16 stations and cluster networks. In brackets, the corresponding number of observed baselines is given, while in the first column the number of possible baselines is shown ($nbas_{max}$)

| ($nbas_{max}$) | S6 | S2 |
|---|---|---|
| 32 Stations (496) | 18 mm (282) | 17 mm (127) |
| 16 Stations (120) | 20 mm (67) | 32 mm (39) |
| Cluster, 20 stat (190) | 15 mm (144) | 10 mm (82) |

With the majority of the observed baselines of lengths between 4,000 and 7,000 km, according to Fig. 3, this only allows observations at elevations below 30° for satellite S2 at 2,000 km orbital height. The severe visibility problem becomes also evident when counting the number of observed baselines, as given in Table 5. With 496 possible baselines, satellite S2 was only observed on 127 baselines. A solution to enable global coverage for S2 observations might be the use of cluster networks. We combined the three regional networks of Sect. 4.1, delivering weekly 3D position rms of a few millimeters (Fig. 11).

When observing the higher orbiting satellite S6, the visibility is much better and the number of observed baselines compared to S2 was nearly doubled for all three networks. The results are about the same for the 32 stations and the 16 stations network, with the latter one shown in Fig. 11. Unfortunately, weekly 3D position rms of up to 30 mm is not very impressive. Best results were again found for the cluster network, though with an expected mean weekly 3D position rms of 15 mm the results are not as good as for the S2 satellite. We see that some of the stations that showed rather bad results, e.g., YAR, suffer from loose connections to the other stations due to their locations at the edge of regional networks. This effect could be mitigated by adding another cluster, e.g., in South America. On the other hand, it is clearly visible that in case of S6 the height component dominates the errors. Considering the strong correlation with the troposphere, this means that the S6 satellite moves too slowly across the sky to enable a good determination of the disturbing troposphere. A combination with common VLBI observations to radio sources, as suggested in the next Sect. (4.3), may be a solution.

Summarizing the results with the global networks, we find that the classical VLBI strategy of using homogeneously distributed stations is very challenging for low satellites.

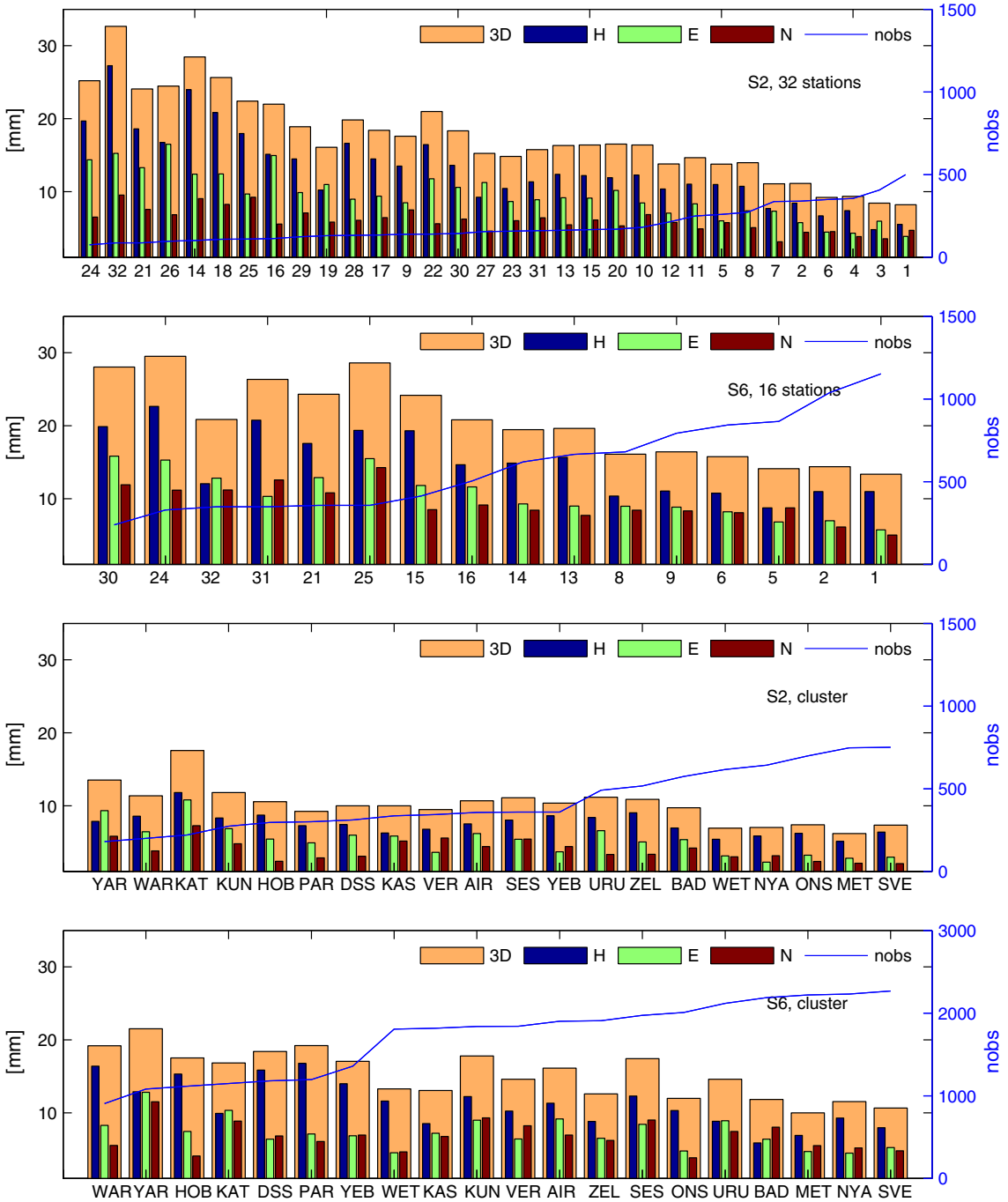


**Fig. 11** Weekly 3D position rms if satellite S2 was observed with a global 32 stations network, satellite S6 with a global 16 stations network, and both satellites in a cluster network comprising 20 real stations. The *blue line* for each station indicates the number of observations per day. The observations were scheduled in 1 min intervals with a cut-off angle of 10°, and the results are given as 3D position rms (*orange*), as well as in the three components height (*blue*), east (*green*) and north (*brown*). The station *numbers of the upper two figures* are those of Fig. 6

Even a fictitious VGOS network comprising 32 stations does not guarantee good results. But, we identified the cluster approach as being very promising. The mixture of short baselines enabling a sufficiently high number of observations together with a global coverage delivers the best results for station coordinates.

### 4.3 Observations to GNSS satellites

VLBI observations to GPS satellites, as one representative of the GNSS, were also tested. When scheduling observations using the same strategy as for satellites S2 and S6, weekly 3D position rms of tens of centimeters was obtained. Although

the common visibility is realized easily compared to satellites S2 and S6, a GPS satellite moves much slower through the sky above a station. In addition, due to its orbital period of 12 sidereal hours, the satellite passes a station only twice per day, on nearly the same track each time. As a consequence, the geometry for the observations does not change from one satellite pass to another, which is necessary to determine good station coordinates and to resolve the troposphere. Hence, alternative strategies for observing GPS satellites with VLBI had to be found. In the following, we shortly introduce two concepts that might be the appropriate approaches.

In the first approach, we combined the observations to one GPS satellite with those of a standard VLBI session to radio sources. Therefore, we merged the schedules of classical radio source observations, as scheduled with VieVS (Sun et al. 2014), with the weekly schedule of one GPS satellite observed with the EUR network. The combination was done without consideration of observation duration or slewing times. As a result, observations to radio sources can be very close in time to those to the satellite, though not at exactly identical epochs. This might not be possible to realize in actual observations, though we found it acceptable for the simulations. In a first step, all observations were used to estimate the tropospheric parameters, and in a second step the radio telescope positions were derived using observations to the GPS satellite only. With this concept, on the one hand the disturbing troposphere is resolved and on the other we got station positions in the satellite system. These positions can be compared in a next step to those determined by classical VLBI.

While the local sky coverage for observations of one single GPS satellite is very poor (only two passes per day), it improves drastically when observations to radio sources are added. In this combined approach, the observations are nearly perfectly distributed (Fig. 12, left). Processing a weekly combined schedule for the EUR network, 3D position rms on the order of 4 mm was achieved. The results are presented in Fig. 13.

Having available the whole GPS constellation instead of a single satellite, obviously there is the option of observing several satellites. We scheduled observations to five GPS satellites in the EUR network, with 2 min intervals. We chose five satellites in a way that not all move in the same orbital plane. The observations of 1 day at station Onsala are visualized in the right skyplot of Fig. 12, indicating that satellites of four different planes were observed. To guarantee fast switching between different targets, every 2 min, a new satellite was observed. This means, that one satellite was observed at most once every 10 min. The result of the weekly solution is shown in Fig. 14, with weekly 3D position rms of 5–10 mm. For all stations, the height errors clearly dominate the accuracy limits, indicating either problems with the troposphere or reduced sensitivity to the height component by the use of the high, slowly moving GPS satellites.

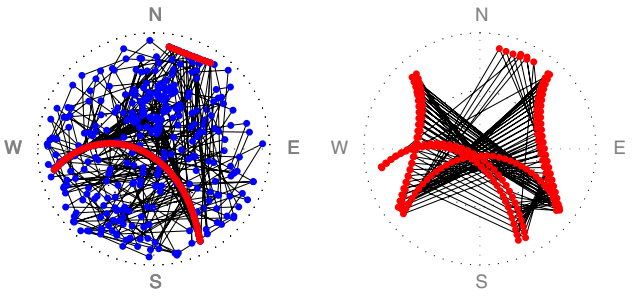


**Fig. 12** Distribution of the observations during 1 day for station Onsala. *On the left*, one satellite was observed in the EUR network with 5 min intervals (*red dots*). The *blue dots* represent the additional observations to extragalactic radio sources in the combined schedule. *On the right*, 1 day of the multi-satellite schedule is visualized for station Onsala. The *black lines* connect consecutive observations

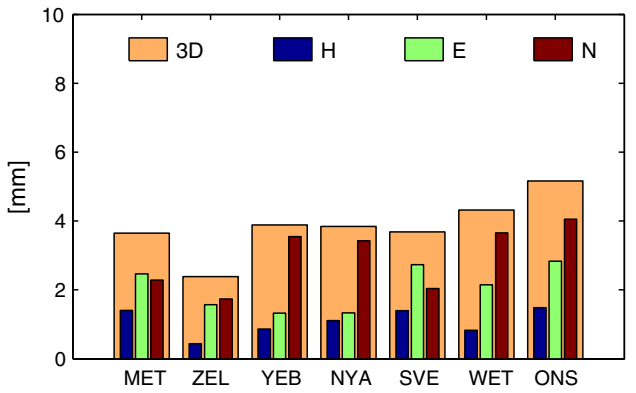


**Fig. 13** Weekly 3D position rms if one GPS satellite was observed in the EUR network with 5 min intervals using the combined approach

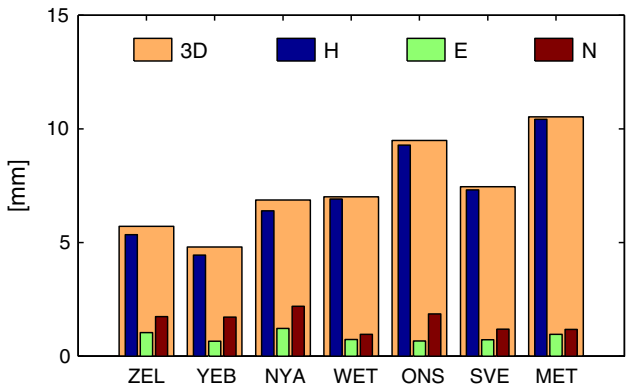


**Fig. 14** Weekly 3D position rms if 5 GPS satellites were observed in the EUR network, applying a scheduling strategy with fast switching between the satellites every 2 min

## 5 Conclusions

With the simulations presented in this paper, we show the possibilities of VLBI observations to satellites. Depending on the satellite orbit, respectively, antenna network, the observing strategies enable the derivation of antenna positions on Earth in the satellite system with a precision of a few millimeters up to 1–2 cm for weekly solutions. For satellites up to orbital heights of 6,000 km, several passes of the satellite above a station per day, together with the concept of the weekly solution compensate the lack of good sky coverage compared to classical VLBI. The today existing antenna infrastructure and the upcoming VGOS systems provide adequate regional and global networks for observing satellites of orbital heights between 2,000 and 6,000 km. Especially, the cluster approach seems to be promising. Assuming full antenna compatibility in terms of tracking and signal reception of the existing IVS network, VLBI observations to a low satellite could immediately deliver useful results, without the necessity to wait for future VGOS stations being installed.

The presented single-target tracking is not suitable for observations to satellites of the GPS. Here, we propose the combination with classical VLBI observations or the tracking of more than one GPS satellite in one session to improve the geometry and to properly resolve the troposphere.

The precise antenna coordinates in the satellite system can further be compared to the coordinates determined by classical VLBI. Possible discrepancies can detect inconsistencies, systematics and technique-specific errors in today's GNSS and VLBI systems.

We showed that with a simple observation setup it is possible to derive promising results. However, concerning the feasibility of a large global network observing one satellite during one week, the implementation of satellite observations into routine sessions will be a difficult topic. Here, also the sandwich-method with sequences of observations to radio source—satellite—radio source, that is commonly applied in VLBI spacecraft tracking, might be an option. This can also help to improve the determination of the troposphere, compared to the approach presented in this paper.

Not treated comprehensively within this study but of major importance is the technical realization of observations to satellites. Hence, adequate receivers have to be developed, capable to observe the signals emitted by the satellite. When also classical observations to radio sources are included in the schedule, hybrid receivers might be necessary, enabling the observation of signals of different strength and/or frequency. For very strong satellite sources, as e.g., the GNSS signals, there is also the danger that the strong satellite signal leaks into the signal of a close extragalactic radio source[4]. Another point is the realization of the complete observation chain, including (1) a scheduling respecting the actual antenna specifications, (2) the development of new data formats accounting also for observations to satellites, (3) the implementation of satellite orbits in the field system of the radio telescope, and (4) a mature data processing, comprising correlation, ambiguity resolution, and data analysis. Concerning the tracking of the satellites, e.g., the SATTRACK module (Moya Espinosa and Haas 2007) could be used.

In this study, we used a simulation method that was found adequate for classical VLBI observations to radio sources. Possible additional error sources, as e.g., the influence of deficient orbit determination of the target satellite or special characteristics of the transmitter, were not included in the investigations above and are recommended to be object of future research.

**Acknowledgments** The presented research was done within project D-VLBI (SCHU 1103/4-1) as part of the DFG Research Unit Space-Time Reference Systems for Monitoring Global Change and for Precise Navigation in Space funded by the German Research Foundation (FOR 1503). We kindly acknowledge four anonymous reviewers for their useful and detailed comments.

[4] V. Tornatore, personal communication.

## References

Altamimi Z, Collilieux X, Métivier L (2011) ITRF2008: an improved solution of the international terrestrial reference frame. J Geod 85(8):457–473

Bar-Sever Y, Haines B, Bertiger W, Desai S, Wu S (2009) Geodetic Reference Antenna in Space (GRASP)—a mission to enhance space-based geodesy. In: COSPAR colloquium: scientific and fundamental aspects of the Galileo program, Padua, 2009

Böhm J, Böhm S, Nilsson T, Pany A, Plank L, Spicakova H, Teke K, Schuh H (2012) The new Vienna VLBI Software VieVS. In: Proceedings of the 2009 IAG symposium, Buenos Aires, Argentina, vol 136. International Association of Geodesy Symposia

Brieß K, Konemann G, Wickert J (2009) MicroGEM—microsatellites for GNSS Earth Monitoring, Abschlussbericht Phase 0/A. Helmholtz-Zentrum Potsdam Deutsches GeoForschungsZentrum GFZ and Technische Universität Berlin

Counselman C, Gourevitch SA (1981) Miniature interferometer terminals for earth surveying: ambiguity and multipath with global positioning system. IEEE Trans Geosci Remote Sens GE 19(4):244–252

Dickey JM (2010) How and why do VLBI on GPS. In: Behrend D, Baver K (eds) International VLBI service for geodesy and astrometry 2010 general meeting proceedings, pp 65–69. NASA/CP 2010–215864

Duev DA, Molera Calvés G, Pogrebenko SV, Gurvits LI, Cim G, Bocanegra Bahamon T (2012) Spacecraft VLBI and Doppler tracking: algorithms and implementation. Astron Astrophys 541:A43. doi:10.1051/0004-6361/201218,885

Hanada H, Iwata T, Namiki N, Kawano N, Asari K, Ishikawa T, Kikuchi F, Liu Q, Matsumoto K, Noda H, Tsuruta S, Goossens S, Iwadate K, Kameya O, Tamura Y, Hong X, Ping J, Aili Y, Ellingsen S, Schlüter W (2008) VLBI for better gravimetry in SELENE. Adv Space Res 42:341–346

Hase H (1999) Phase centre determinations at GPS-satellites with VLBI. In: Schlüter W, Hase H (eds) Proceedings of the 13th working meeting of the European VLBI for geodesy and astrometry, Bundesamt für Kartographie und Geodäsie, Wettzell, pp 273–277, held at Viechtach

Hase H, Behrend D, Ma C, Petrachenko B, Schuh H, Whitney A (2013) The emerging VGOS network of the IVS. In: Behrend D, Baver K (eds) International VLBI service for geodesy and astrometry 2012 general meeting proceedings, pp 8–12. NASA/CP-2012-217504

Huang Y, Hu X, Huang C, Jiang D, Zheng W, Zhang X (2006) Orbit determination of satellite "Tance 1" with VLBI data. Chin Astron Astrophys 30:318–329

Huang Y, Hu X, Zhang X, Jiang D, Guo R, Wang H, Shi S (2011) Improvement of orbit determination for geostationary satellites with VLBI tracking. Chin Sci Bull 56:2765–2772

Klioner SA (1991) General relativistic model of VLBI observables. In: Proceedings of the AGU Chapman conference on geodetic VLBI: monitoring global change, pp 188–202. NOAA Technical Report NOS 137 NGS 49

Kwak Y, Gotoh T, Amagai J, Takiguchi H, Sekido M, Ichikawa R, Sasao T, Cho J, Kim T (2010) The first experiment with VLBI-GPS hybrid system. In: Behrend D, Baver K (eds) International VLBI service for geodesy and astrometry 2010 general meeting proceedings, pp 330–334. NASA/CP 2010–215864

Lanyi G, Bagri DS, Border JS (2007) Angular position determination of spacecraft by radio interferometry. Proc IEEE 95:11

Lebreton JP, Witasse O, Sollazzo C, Blancquaert T, Couzin P, Schipper AM, Jones JB, Matson DL, Gurvits LI, Atkinson DH, Kazeminejad B, Pérez-Ayúcar M (2005) An overview of the descent and landing of the Huygens probe onTitan. Nature 438(8):758–764. doi:10.1038/nature04347

MacMillan DS, Ma C (1994) Evaluation of very long baseline interferometry atmospheric modeling improvements. J Geophys Res 99(B1):637–651

Moya Espinosa M, Haas R (2007) SATTRACK a satellite tracking module for the VLBI field system. In: Böhm J, Pany A, Schuh H (eds) Proceedings of the 18th European VLBI for geodesy and astrometry working meeting, Vienna, vol 79, pp 53–58. Schriftenreihe der Studienrichtung Vermessung und Geoinformation, Technische Universität Wien, ISSN 1811-8380

Moyer TD (2003) Formulation for observed and computed values of deep space network data types for navigation. In: Yuen JH (ed) JPL deep space communications and navigation series. Wiley, New York, ISBN: 0-471-44535-5

Niell AE (2007) Simulation networks-1. IVS Memorandum 2007-001v01. ftp://ivscc.gsfc.nasa.gov/-pub/memos/ivs-2007-001v01.pdf

Nilsson T, Haas R, Elgered G (2007) Simulations of atmospheric path delays using turbulence models. In: Böhm J, Pany A, Schuh H (eds) Proceedings of the 18th European VLBI for geodesy and astrometry working meeting, 12–13 April 2007, Vienna, vol 79, pp 175–180. Schriftenreihe der Studienrichtung Vermessung und Geoinformation, Technische Universität Wien, ISSN 1811–8380

Pany A, Böhm J, MacMillan DS, Schuh H, Nilsson T, Wresnik J (2010) Monte Carlo simulations of the impact of troposphere, clock and measurement errors on the repeatability of VLBI positions. J Geod 85(1):39–50

Petrachenko B, Niell A, Behrend D, Corey B, Böhm J, Charlot P, Collioud A, Gipson J, Haas R, Hobiger T, Koyama Y, MacMillan D, Malkin Z, Nilsson T, Pany A, Tuccari G, Whitney A, Wresnik J (2009) Progress report of the IVS VLBI2010 committee: design aspects of the VLBI2010 system. NASA/TM-2009-214180. ftp://ivscc.gsfc.nasa.gov/pub/misc/V2C/TM2009-214180.pdf

Preston RA, Ergas R, Hinteregger HF, Knight CA, Robertson DS, Shapiro II, Whitney AR, Rogers AEE, Clark TA (1972) Interferometric observations of an artificial satellite. Science 178–4059:407–409

Rosenbaum B (1972) The VLBI time delay function for synchronous orbits. NASA/TM-X-66122 GSFC

Sarti P, Abbondanza C, Petrov L, Negusini M (2011) Height bias and scale effect induced by antenna gravitational deformations in geodetic VLBI data analysis. J Geod 85:1–8. doi:10.1007/s00190-010-0410-6

Schuh H, Behrend D (2012) VLBI: a fascinating technique for geodesy and astrometry. J Geodyn 61:68–80

Seitz M, Angermann D, Bloßfeld M, Drewes H, Gerstl M (2012) The 2008 DGFI realization of the ITRS: DTRF2008. J Geod 86(12):1097–1123

Sun J (2013) VLBI scheduling strategies with respect to VLBI2010. Dissertation, Geowissenschaftliche Mitteilungen 92, Schriftenreihe der Studienrichtung Vermessung und Geoinformation, Technische Universität Wien, ISSN 1811–8380

Sun J, Böhm J, Nilsson T, Krásná H, Böhm S, Schuh H (2014) New VLBI2010 scheduling strategies and implications on the terrestrial reference frames. J Geod. doi:10.1007/s00190-014-0697-9 (in press)

Thaller D, Dach R, Seitz M, Beutler G, Mareyen M, Richter B (2011) Combination of GNSS and SLR observations using satellite colocations. J Geod 85:257–272

Tornatore V, Haas R (2009) Considerations on the observation of GNSS-signals with the VLBI2010 system. In: Bourda G, Charlot P, Collioud A (eds) Proceedings of the 19th European VLBI for geodesy and astrometry working meeting. Université Bordeaux 1-CNRS Observatoire Aquitain des Sciences de l'Univers Laboratoire d'Astrophysique de Bordeaux, pp 151–155, Bordeaux

Tornatore V, Haas R, Duev D, Pogrebenko S, Casey S, Molera Calvés G (2011) Determination of GLONASS satellite coordinates with respect to natural radio sources using the VLBI technique: preliminary results. In: Association Astronautique et Aéronautique de France e SEE (Société de l'Electricité, de l'Electronique et des Technologies del'Information et de la Communication) (ed) ETTC2011, European test and telemetry conference, Toulouse. http://publications.lib.chalmers.se/records/fulltext/local_-150623.pdf